

# Elemental carbon deposition to Svalbard snow from Norwegian settlements and long-range transport

By BORGAR AAMAAS<sup>1,2,\*</sup>, CARL EGEDE BØGGILD<sup>2</sup>, FRODE STORDAL<sup>1</sup>,  
TERJE BERNTSEN<sup>1,3</sup>, KIM HOLMÉN<sup>2,4</sup> and JOHAN STRÖM<sup>4,5</sup>, <sup>1</sup>University of Oslo, UiO, P.O. Box  
1072, Blindern, N-0316 Oslo, Norway; <sup>2</sup>The University Centre in Svalbard, UNIS, P.O. Box 156, N-9171  
Longyearbyen, Norway; <sup>3</sup>Center for International Climate and Environmental Research – Oslo, Cicero, P.O. Box  
1129, Blindern, N-0318 Oslo, Norway; <sup>4</sup>Norwegian Polar Institute, NPI, Polar Environmental Centre, N-9296 Tromsø,  
Norway; <sup>5</sup>Stockholm University, SE-106 91 Stockholm, Sweden

(Manuscript received 3 July 2010; in final form 3 March 2011)

## ABSTRACT

The impact on snow pack albedo from local elemental carbon (EC) sources in Svalbard has been investigated for the winter of 2008. Highly elevated EC concentrations in the snow are observed around the settlements of Longyearbyen and Svea (locally  $>1000 \text{ ng g}^{-1}$ , about 200 times over the background level), while EC concentrations similar to the background level are seen around Ny-Ålesund. Near Longyearbyen and Svea, darkened snow influenced by wind transported coal dust from open coal stockpiles is clearly visible from satellite images and by eye at the ground. As a first estimate, the reduction in snow albedo caused by local EC pollution from the Norwegian settlements has been compared to the estimated reduction caused by long-range transported EC for entire Svalbard. The effect of local EC from Longyearbyen, Svea and all Norwegian settlements are estimated to 2.1%, 7.9% and 10% of the total impact of EC, respectively. The EC particles tend to stay on the surface during melting, and elevated EC concentrations due to the spring melt was observed. This accumulation of EC enhances the positive albedo feedbacks. The EC concentrations were observed to be larger in metamorphosed snow than in fresh snow, and especially around ice lenses.

## 1. Introduction

The most effective light absorbing particle reducing snow albedo per mass is soot, often referred to as black carbon (BC), which is about 50 times more effective than dust (Warren, 1984). In this study, elemental carbon (EC) is measured as a proxy of BC. Due to the coal mining industry in Svalbard, EC will also be a proxy of coal dust concentrations in Svalbard snow. Soot is black or blackish particles that are produced by incomplete combustion processes of fossil fuel, biofuel or biomass; hence, from both natural and anthropogenic sources. Coal dust is created during mining, transportation and mechanical handling of coal. Coal is geologically processed organic matter that turned black in the making (Bond and Bergstrom, 2006). Warren and Wiscombe (1980) were the first to quantify a relation between BC concentrations and reduction in snow albedo by modelling. Since snow

is weakly absorptive in the visible wavelengths and BC is highly absorptive and multiple scattering occurs in the snow pack, the spectral snow albedo is reduced by even small concentrations of BC for wavelengths  $\lambda < 0.9 \mu\text{m}$  (Warren and Wiscombe, 1980).

Several positive feedbacks magnify the initial warming due to BC in snow. The presence of BC will trigger and enhance the snow-albedo feedback and the warming-induced snow grain growth feedback, in addition to increased snow grain growth due to heating caused by BC in the snow (Flanner et al., 2007). During melting, a majority of the hydrophobic and large BC particles will stay in the snow surface, while most of the hydrophilic BC particles will be flushed out (Conway et al., 1996; Flanner et al., 2007). In total, the BC concentration in the surface snow is increased. The global radiative forcing of BC in snow has been modelled by Flanner et al. (2007) and Rypdal et al. (2009) to be  $0.054 \text{ W m}^{-2}$  and  $0.03 \text{ W m}^{-2}$ , respectively. Due to the strong feedbacks, the ‘efficacy’ is high, resulting in a temperature response from the forcing of about 1.7–4.5 times that of a similar forcing from atmospheric  $\text{CO}_2$  (Hansen et al., 2005; Flanner et al., 2007). The maximum zonally averaged forcing has been predicted to reach almost  $1.5 \text{ W m}^{-2}$  in the

\*Corresponding author.

Center for International Climate and Environmental Research – Oslo,  
Cicero, P.O. Box 1129 Blindern, N-0318 Oslo, Norway.  
e-mail: borgar.aamaas@cicero.uio.no  
DOI: 10.1111/j.1600-0889.2011.00531.x

Arctic during the spring snow melt (Flanner et al., 2007), while a temperature response of about 0.5 °C in the Arctic throughout the year is estimated (Quinn et al., 2008). Flanner et al. (2009) modelled that 20% of the snow darkening forcing in spring is caused by mineral dust, the rest by BC.

BC particles in the atmosphere are typically 0.01–0.4 µm in size (Bond et al., 2006), which are mainly removed by wet fall-out (Vignati et al., 2010) after an average atmospheric lifetime of 7.3 days (Schulz et al., 2006). Due to this short lifetime, only a limited amount of the worldwide BC pollution reaches Svalbard (Stohl, 2006). Only a small fraction of the emissions occur in the Arctic (Bond et al., 2004). In addition, the Arctic front (Law and Stohl, 2007) isolates the Arctic from the warmer mid-latitudes. Long-range transported BC pollution is mainly transported to Svalbard from Europe and Northern Asia (Stohl, 2006; Reddy and Boucher, 2007; Shindell et al., 2008). Forsström et al. (2009) observed that air arriving from the east into Svalbard contained the most BC inferred from snow samples and trajectory models, which supports the find of Eleftheriadis et al. (2009) that the heavily polluted air masses measured at the Zeppelin station in Svalbard originate from Northern and Central Russia. BC concentrations in the air show a high monthly variability with the maximum observed in February and March at Zeppelin. Events with higher concentrations are seen all-year around, although the most pronounced in winter and spring in connection with the observed Arctic Haze (Rosen et al., 1981; Shaw, 1995; Eleftheriadis et al., 2009). Hence, transport of BC to Svalbard is caused by transport events superimposed on a distinct seasonal cycle.

We know of only two published studies that have measured the background level of BC or EC in snow in Svalbard. Clarke and Noone (1985) measured a BC mean of 30 ng g<sup>-1</sup> for its Svalbard samples, while Forsström et al. (2009) used the same analysis method as in this study and found the median background EC concentrations for Svalbard to be 4.1 ng g<sup>-1</sup>. The difference in the analysis methods can partly explain the gap between the results (Watson et al., 2005).

Other light-absorbing impurities are also observed in the snow pack. The first author has often observed brownish snow in Svalbard discoloured by Aeolian sediments. A yearly deposition of Aeolian sediments in the terrain and climate like Svalbard is typically 11 g m<sup>-2</sup> (Owens and Slaymaker, 1997); however, values as high as 270–400 g m<sup>-2</sup> have been measured in some parts of Svalbard (Czeppe, 1966; Åkerman, 1980). If we assume that all the sediments are mixed into the snow with a mean snow pack in Svalbard of 686 mm w.e. (Winther et al., 1998), the dust concentration is roughly 16 µg g<sup>-1</sup>. This concentration is three orders of magnitude larger than the background EC concentration.

Svalbard, an archipelago in the European High Arctic, is defined as all land masses between the latitudes of 74 and 80 °N and longitudes 10 and 35 °E. The total land area is 61 000 km<sup>2</sup>, comparable in size to Ireland. There are only a few settlements in

Svalbard. Longyearbyen (population: 2100) is the largest town. Some coal mining is present, and the town is electrified by a coal and diesel power plant. Svea (240) is an active coal mining town with its own diesel power plant. Coal is transported in trucks from the mine to a coal stockpile at Cape Amsterdam, a distance of about 9 km. Several thousand tons of coal is stored at this stockpile at any given time. Ny-Ålesund (30–150) is a research settlement with its own small diesel power plant. The Russian settlement of Barentsburg (500) is a coal mining town with an uncleaned coal power plant. In addition, some smaller research stations are situated in the archipelago. Marine transportation around Svalbard is the largest BC combustion source (coal dust not included) compared to other sectors (Vestreng et al., 2009).

Only a few studies have investigated how local sources affect BC concentrations in snow in otherwise pristine areas, such as in Antarctica (Warren and Clarke, 1990; Grenfell et al., 1994), the Arctic Ocean (Grenfell et al., 2002) and Greenland (Hagler et al., 2008). In Svalbard, no such study has been done for BC in snow; however, accelerated melting near Longyearbyen has been linked to extremely high BC concentrations (Bøggild et al., 2007). Jaedicke (2002) remarked that Adventdalen, a valley close to Longyearbyen, is one of the first places on Svalbard to be snow free in the spring. The local effects from some other pollutants have been studied in Svalbard (Beine et al., 1996), and high local pollution levels have been measured (Reimann et al., 2009). Aeolian transport of coal dust from coal stockpiles and open coal pit mines has been thoroughly investigated and modelled (Jones et al., 2002; Naidoo and Chirkoot, 2004; Ghose and Majee, 2007); however, a quantification of the albedo reduction due to the coal dust in snow has to our knowledge never been reported before.

In this study, the effects of local EC pollution are investigated and compared to the impact from long-range transported EC that form the EC background level in Svalbard. The EC concentration in the snow pack has been measured around settlements. The climatic impact is estimated according to the first-order snow albedo reduction caused by the varying EC concentrations. From this, a first estimate of the significance of the local pollution is calculated.

## 2. Methods

### 2.1. Snow sampling and chemical analysis

A total of 196 samples of snow were analysed. Snow was sampled from radial transects in valley floors with origin in Longyearbyen, Ny-Ålesund and Svea. Snow pits were excavated with 1–5 km intervals. Snowmobiles and cars were left downwind and preferably 100 m from the sites to minimize contamination risk. Up to five snow samples were collected where each sample represents one part of the snow column at the site. Layer 1 is defined as the bottom layer. Normally, about 1.2 kg of snow was needed for the chemical analysis, less for heavily polluted snow.

The snow was melted in a microwave oven and immediately filtered through a quartz filter. Some of the hydrophobic EC might stick to the sample jar after melting; however, Forsström et al. (2009) found that with an identical setup as in this study, a significant loss of EC required the sample to be stored in liquid form for at least 1.5 d. Further, the quartz filter will not capture all the submicrometer EC. Ogren et al. (1983) observed a filtration efficiency of 50–80% compared to a polycarbonate membrane filter. Three of our samples were filtered twice with the same water to investigate the efficiency of the filtration. The second filter had undetectable amounts EC in two of the cases, while the efficiency was about 70% for the last sample. This loss of EC in some of the samples introduces an uncertainty and gives an equivalent underestimate of the EC concentrations. The Thermal/Optical Carbon Aerosol Analyzer (Sunset Laboratory Inc., Forest Grove, USA) with NIOSH 5040 protocol (Birch, 2003) was used to measure EC concentrations in the snow. In the first step of the analysis, the OC is volatilized at temperatures up to 820 °C in a pure helium atmosphere. The second heating up to 860 °C in an oxygen (10%)–helium mixed atmosphere burns the EC. The evolved carbon is oxidized to CO<sub>2</sub> and, finally, reduced to CH<sub>4</sub>, which is detected by a flame ionization detector (FID). Pyrolysis during the analysis is corrected for by the monitoring of the filter transmittance. Studies on air samples by Chow et al. (2001) and Reisinger et al. (2008) has shown that the NIOSH 5040 protocol may underestimate the EC content because mineral oxides on the sample may provide oxygen already in the first step of the analysis. Therefore, some of the EC is attributed to the OC fraction. Chow et al. (2001) compared the NIOSH 5040 protocol to the IMPROVE protocol (Chow et al., 1993). The authors got an average ratio IMPROVE/NIOSH 5040 of 3.45 (for significant data points). Reisinger et al. (2008) compared the NIOSH 5040 protocol to a modified NIOSH protocol called NIOSH (A3) where the temperature for the high temperature stage of the He atmosphere step was lowered from 870 to 550 °C. The authors found an average ratio NIOSH (A3)/NIOSH 5040 of 1.48. A similar study has not been published for snow samples that were melted; however, our own experiments comparing IMPROVE with NIOSH 5040 are in line with the previous studies for air (Reisinger et al., 2008) and indicate that method IMPROVE shows systematic higher estimates compared with method NIOSH 5040 by a factor of 2. Birch and Cary (1996) determined a lower limit of detection of 0.23  $\mu\text{g C cm}^{-2}$ . Using the typical volume of melted snow (1.2 L), this corresponds to a concentration of about 2  $\text{ng g}^{-1}$ . Concentrations on blank filters were typically less than 0.05  $\mu\text{g cm}^{-2}$ , which corresponds to about 0.4  $\text{ng g}^{-1}$ .

## 2.2. Weather data

Temperature and wind data were studied to better understand the snow stratigraphy and the airborne transport of EC from local sources. Observations from stations operated by the Nor-

wegian Meteorological Institute during the period from September 2007 to April 2008 have been used (Longyearbyen Airport, Ny-Ålesund and Sveagruva). The data are available at <http://www.eklima.no>.

## 2.3. Calculating the EC budget for Svalbard

A first estimate of the significance of local EC pollution was calculated based on the direct snow albedo reduction from varying EC concentrations. The measured EC concentrations were linked to the modelled reductions in the snow surface albedo for the 350–2500 nm wavelength band. Values from Rypdal et al. (2009) were used to link EC concentration to snow albedo for different spectral bands. That study used radiative transfer code as in Stamnes et al. (1988) and the optical EC properties as found by Bond et al. (2006). To get the total snow albedo, these data were applied to an incident spectral irradiance spectrum for clear skies given by Grenfell and Perovich (2004, fig. 11). A relation between EC concentration and reduced snow albedo is, hence, established.

The optical snow grain radius is set to 0.5  $\mu\text{m}$ , while the optical EC particle size distribution is given as a simple modal size distribution with a standard deviation of 2 in the model (Rypdal et al., 2009). These parameters are used since we have not measured the EC particle sizes. In general, soot particles in the atmosphere have typically a size of 0.2  $\mu\text{m}$  (Bond et al., 2006), while coal dust particles are generally larger (typically between 3 and 20  $\mu\text{m}$  (Jones et al., 2002; Naidoo and Chirkoot, 2004; Ghose and Majee, 2007)). In areas near open coal stockpiles and transportation routes of coal, most of the measured EC is coal dust. According to Warren and Wiscombe (1980, Fig. 4b), the larger particles as coal dust will be about a factor of 5 times less effective at reducing snow albedo than soot particles. Hence, this method will overestimate the albedo effect for these areas. This source of error is discussed later.

The goal is to estimate the snow albedo impact from each Norwegian settlement in Svalbard, as explained in this paragraph. According to the modeled EC–snow albedo relation, the typical background EC concentration of 4.1  $\text{ng g}^{-1}$  in Svalbard (Forsström et al., 2009) would lower the direct snow albedo by 0.0011. A representative EC concentration for every sample site was based on the mean EC concentration of the site's samples, which minimizes the impact of natural variability of EC in the snow pack. This snow albedo reduction was derived using the modelled relationship as described. The EC concentration in snow is typically elevated around the settlements and decreasing with distance from the settlements until the background concentration is met. By looking at transects going out from the settlements, areas observed to be affected by local EC emissions were detected. For all sites around Longyearbyen, the EC background level is assumed to be in line with the general mean of 4.1  $\text{ng g}^{-1}$  found by Forsström et al. (2009). The EC background level around Svea is set higher at 9.0  $\text{ng g}^{-1}$  since

Forsström et al. (2009) measured  $9.8 \text{ ng g}^{-1}$  at the background site nearest Svea and the remote samples around Svea in our study have similar EC concentrations. An EC concentration of  $9.0 \text{ ng g}^{-1}$  will reduce the snow albedo by 0.0022. No clear sign of elevated EC concentration levels are seen in the mean values at the sites around Ny-Ålesund. Thus, all the EC around Ny-Ålesund is assumed to be long-range transported, even though local pollution cannot be ruled out. Through this procedure, cut-off values to separate local and long-range transported EC are established. For the sites around Longyearbyen (Svea), the first 0.0011 (0.0022) reduction in snow albedo is, hence, classified as a result of long-range transported EC. If the total reduced snow albedo at a site is higher than this value, the remaining albedo reduction is accounted as a result of local pollution. Every snow pit site was assumed to represent its surrounding area A, which is assumed to cover halfway to the next site by applying the Thiessen method (Boots, 1980) and the width of the valley floor. We assume that the local emissions are not transported upwards into the mountains surrounding all the settlements; hence, this is a conservative pollution dispersion estimate. From this, the effect of local EC pollution from the different settlements was estimated, and a budget for entire Svalbard was calculated. The ratio between the snow albedo impact from local ( $L$ ) EC from settlement  $i$  over all pollution [the sum of long-range transported (LRT) and local] for entire Svalbard is expressed as

$$\frac{L_i}{\sum_i L_i + \text{LRT}} = \frac{\sum_j A_{i,j}(\Delta\alpha_{i,j} - \Delta\alpha_{i,j}^{\text{LRT}})}{\sum_j A_{i,j} \times \Delta\alpha_{i,j}}.$$

The denominator on the left-hand side is the total albedo reduction for Svalbard for all sources. The subscript  $i$  is for settlement,  $j$  is for an area  $A$  that represents the area around the point measurements,  $\Delta\alpha$  is the reduced snow albedo due to EC, and the superscript LRT represents the EC level caused by long-range transported pollution. In areas not affected by EC pollution from any of the settlements,  $\Delta\alpha_{i,j} - \Delta\alpha_{i,j}^{\text{LRT}} = 0$ . A best estimate of the local impact was calculated from this equation. Since coal dust particles are less effective at reducing snow albedo than soot particles due to particle size differences, a low estimate is derived where this is accounted for. Around Svea, we assume that all EC is coal dust, which we estimate will reduce the snow albedo impact by 80%. The EC measured on Longyearbreen is unlikely depositions of coal dust due to its much higher elevation than the coal dust sources around Longyearbyen. Hence, we assume that the level measured there ( $17 \text{ ng g}^{-1}$ ) is representative for the soot concentration around Longyearbyen, while EC concentrations above that are assumed to be coal dust with a 80% lower impact on the albedo. Some possibly affected areas by local pollution, the rugged mountains and slopes around Longyearbyen and Svea, were not measured due to inaccessibility. The areas covered by these mountains are larger than the EC polluted valleys around the settlements. A higher estimate was derived when an EC concentration similar

to that measured in our high altitude samples (Longyearbreen) are included in those areas. The estimate was also calculated separately for the case of snow covered sea ice covering Isfjorden to assess the potential maximum impact local EC sources could have. Van Mijenfjorden near Svea was frozen over at the time of the field work; hence, the albedo impact from this fjord is included in the best estimate.

### 3. Results and discussion

#### 3.1. EC concentrations

The EC measurements around the settlements are presented here, first from Longyearbyen. Extreme levels of EC concentrations were observed locally around Longyearbyen and Svalbard Airport, as seen in Figs 1 and 2. The figures indicate the west–east gradient, showing clearly that local sources are affecting the EC concentrations in the snow pack. Several samples contained concentrations of  $>1000 \text{ ng g}^{-1}$ , while other samples contained too much coal dust to even be analysed (as explained later). Hence, the highest concentrations are even higher than indicated here and likely up to 1% of total mass (Bøggild et al., 2007). The most contaminated snow was found around the coal processing plant 3 km northwest of Longyearbyen, and the snow is visually clearly darkened from this. The average EC concentration was somewhat higher for samples taken in February 2008 than April 2008, since these samples were gathered a bit closer to the trucking road between the mine and the settlement. In the valley of Adventdalen between the town and the coal mine, 5–15 km east of Longyearbyen, the EC concentration is about  $50 \text{ ng g}^{-1}$ . Further east, the concentration decreases with distance until the background level is seen about 50 km to the east of Longyearbyen. No samples could be taken more than 10 km west of Longyearbyen due to the open waters of Isfjorden. The wind was from the southeast ( $90^\circ$ – $180^\circ$ ) 60.0% of the time between the first snow fall and the sampling period at Svalbard Airport, which matches well with the plumes observed downwind of the coal stockpiles.

From Longyearbyen in the north to the glacier Longyearbreen in the south, another plume transect was sampled (Fig. 3). Longyearbreen is situated between 4 and 8 km south of Longyearbyen at a height of 300–600 m a.s.l. The mean concentration on the glacier is  $17 \text{ ng g}^{-1}$ , which is much lower than what is seen in Adventdalen, but considerably over the background level. A large melt event occurred on 1 and 2 January 2008, which resulted in several thick ice lenses on the lower part of the glacier. Elevated EC concentrations were observed in those ice layers similar to what was found by Conway et al. (1996). The sampling was done in April 2008, coinciding with the snowmobile peak season (Reimann et al., 2009). That affected the top snow layer, and the exhaust led to elevated concentrations measured in that snow layer. In addition, snow samples were gathered in August 2009 with a mean concentration of  $231 \text{ ng g}^{-1}$ . While

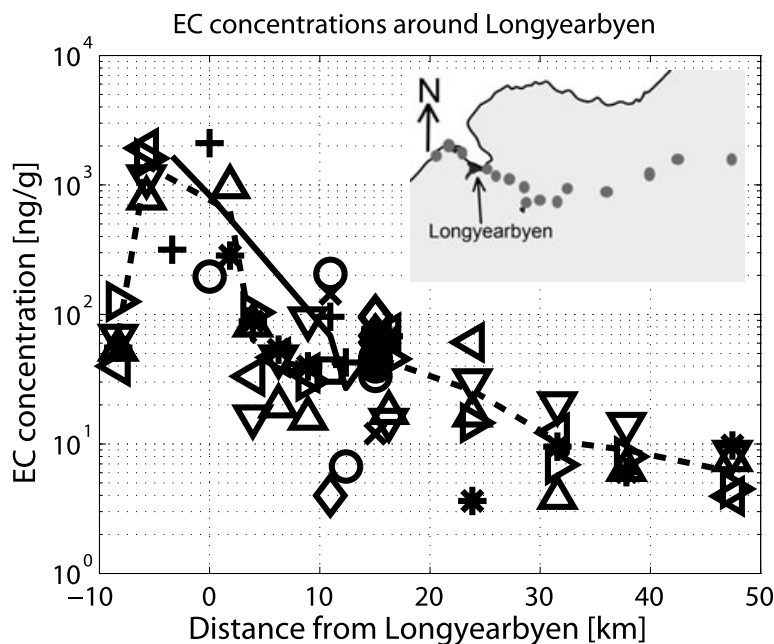


Fig. 1. The EC concentration around Longyearbyen along a east-west transect. Snow samples were gathered from Adventdalen and Sassendalen to the east and on Hotellneset and towards Bjørndalen to the west, as indicated by grey circles in the small map. Layer 1 is the bottom layer in the snow pack. The samples taken in February are marked by plus signs for layer 5, circles for layer 4, crosses for layer 3, squares for layer 2, diamonds for layer 1 and a solid line for the mean. For the April samples, asterisks show layer 5 samples, upward-pointing triangles for layer 4, downward-pointing triangles for layer 3, left-pointing triangles for layer 2, right-pointing triangles for layer 1 and a dashed line for the mean.

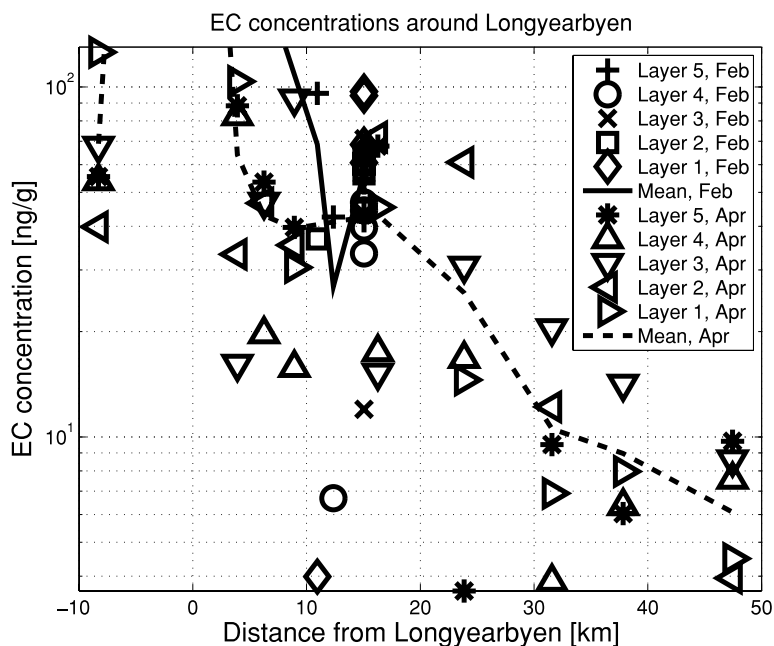


Fig. 2. As Fig. 1, but only for EC concentrations less than  $130 \text{ ng g}^{-1}$ .

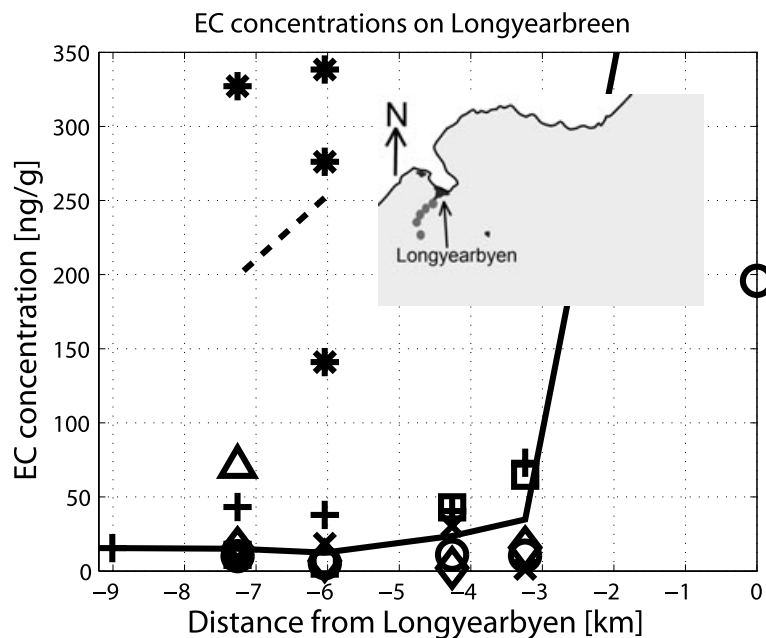
the top layer had an EC concentration, which was a factor of 19 of the mean April concentration, the rest of the snow pack contained a factor of 4 EC. The total EC burden ( $EC_{\text{tot}}$ ) in a snow column is

$$EC_{\text{tot}} = \sum_i (con_i \times d_i \times \rho_i),$$

where  $con$  is the EC concentration,  $d$  the thickness and  $\rho$  the snow density for each  $i$  snow layer. The total EC burden for the snow column in April is estimated to  $9.1 \text{ mg m}^{-2}$  with a

typical snow density of  $0.37 \text{ g cm}^{-3}$  (Winther et al., 1998). In August, the EC burden has increased to  $15 \text{ mg m}^{-2}$  with an estimated density of  $0.5 \text{ g cm}^{-3}$  for wet summer snow and  $0.85 \text{ g cm}^{-3}$  for superimposed ice (Tedesco et al., 2009). The superimposed ice is assumed to be about 10 cm thick (Hagen and Liestøl, 1990). The increase in EC burden indicates that most of the EC particles initially present in April were not removed. If we assume that the wet deposition of EC is proportional to the precipitation amount and that dry deposition from long-range transported sources is minimal relative to wet deposition

Fig. 3. The EC concentration along a northsouth transect near Longyearbyen at sites indicated by grey circles in the map. The three sampling sites that are located between 4 and 8 km south of Longyearbyen are found on the glacier Longyearbreen. The snow was sampled in April 2008 and August 2008. The samples taken in April are marked by plus signs for layer 5, circles for layer 4, crosses for layer 3, squares for layer 2, diamonds for layer 1 and a solid line for the mean. The samples from August are marked by asterisks for layer 5, upward-pointing triangles for layer 4 and a dashed line for the mean.



(Vignati et al., 2010), about 80% of the burden increase can be accounted for by deposition from precipitation between April and August when the precipitation measurements at Svalbard Airport are considered. The rest of the increase is likely from the extensive snowmobile traffic around the site from April to June. In conclusion, most of the EC particles stayed on the snow surface during the spring melt, as observed by Conway et al. (1996), and additional EC is brought to the surface from precipitation, dry fallout and local pollution during spring and summer.

Around Ny-Ålesund, local EC pollution in the snow is difficult to observe (see Fig. 4). The mean concentration of  $6.6 \text{ ng g}^{-1}$  is near the background EC concentration of Svalbard; however, the variability is large with a standard deviation of  $4.3 \text{ ng g}^{-1}$ . Local pollution cannot be ruled out completely since some of the samples contained up to  $15 \text{ ng g}^{-1}$ . The plume from the power plant in Ny-Ålesund is typically drifting to the northwest since the wind was southeasterly 61% of the time at the meteorological station during the period when there was snow on the ground prior to the snow sampling. Hence, the plume drifts mostly over Kongsfjorden. No sea ice was observed during the sampling period; hence, no snow samples could be taken directly downwind of Ny-Ålesund.

In Svea, the EC concentrations in the snow are similar to what was measured around Longyearbyen (see Figs 5 and 6). Near Svea, the concentration is above  $1000 \text{ ng g}^{-1}$ , but drops rapidly with increasing distance. The background level is approached some 20–30 km away from the settlement. Large amounts of available coal dust are causing these extreme EC concentrations. Since the coal dust particles are much coarser than the soot particles, they are carried to a shorter distance, which give

rise to the large gradient seen. A distinct black plume is seen downwind of the coal stockpile on Cape Amsterdam, it can even be seen in satellite images (see Fig. 7). The wind direction at the meteorological station in Svea was mainly northeasterly with occasional periods of southwesterly winds during the winter. The coal dust content in the snow adjacent to this coal stockpile has previously been measured by Myhr (2003) to vary between 79 and  $313 \mu\text{g g}^{-1}$ . That is two orders of magnitude larger than any of the EC measurement in this work, indicating that the EC concentrations are underestimated in highly coal dust affected areas in this study (as explained later). Van Mijenfjorden is situated west and southwest of Svea, and this fjord freezes during winter. No snow samples were taken from the sea ice due to safety precautions. Hence, coal dust can easily spread over a large flat area of snow with no obstacles and, thus, have a significant climatic impact on snow and ice covered areas.

A micro scale study was performed as part of the sampling southeast of Longyearbyen (see Fig. 8). Snow was sampled from four vertical profiles along a 5-m-long transect. The same snow profiles along a 5-m-long transect. The same snow layers in the four snow pits were sampled with the help of snow stratigraphy investigations. The mean value of all 20 samples was  $57 \text{ ng g}^{-1}$  with a standard deviation that was 35% of that value. The spatial variability between the snow pits was small with a standard deviation of 5.9%. In comparison, the standard deviation of all samples gathered around Ny-Ålesund, a place with low EC concentration, was 68% of the mean. The EC concentrations in multiple samples from the same location can vary by a factor of 2 at very low EC concentrations (Forsström et al., 2009), since instrumental errors have an increasing relative impact for decreasing EC concentrations. Overall, the variability seen is mainly a result of variability in EC concentrations in

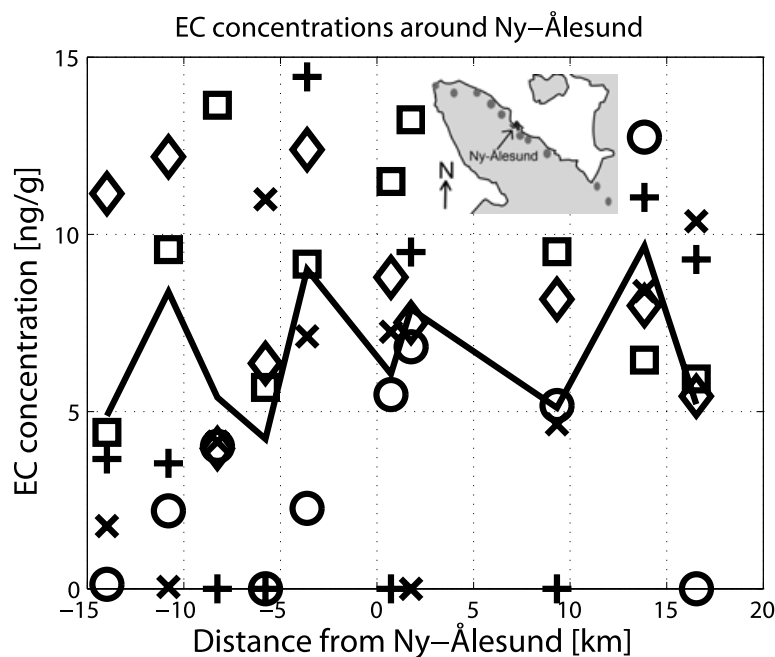


Fig. 4. EC concentration in a northwest–southeast directed transect near Ny-Ålesund. Positive values are in southeasterly direction. The samples were taken on land parallel to Kongsfjorden in March 2008 at sites shown as grey circles in the map. The samples are marked by plus signs for layer 5, circles for layer 4, crosses for layer 3, squares for layer 2, diamonds for layer 1 and a solid line for the mean.

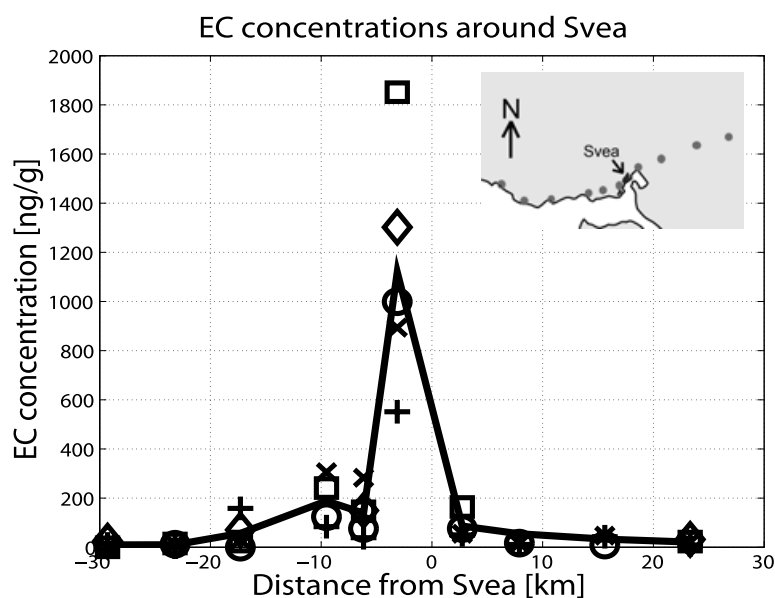


Fig. 5. EC concentration in a west–east transect around Svea. Positive values indicate east. The samples were collected in March 2008 at the sites given by the grey circles in the map. The samples are marked by plus signs for layer 5, circles for layer 4, crosses for layer 3, squares for layer 2, diamonds for layer 1 and a solid line for the mean.

the snow pack caused by small-scale processes. Snow is often drifting in Svalbard (Jaedicke, 2001), and snow from individual snow events is, then, mixed heterogeneously. This mixing explains the large variability in EC concentration measured for the vertically separated snow layers (standard deviation: 25%). Low-density snow will start to drift when the wind speed at 10 m reaches  $1.9 \text{ m s}^{-1}$  and for wind-hardened snow  $10.5 \text{ m s}^{-1}$  (Male, 1980). Those thresholds were exceeded 87% and 9.0% of the time, respectively, during the winter of 2007/08 at Svalbard Airport. The numbers are similar in Ny-Ålesund and

Svea. Hence, snow drift and mixing of snow occur often. This mixing makes sampling of snow from individual precipitation events difficult.

Several samples were sampled at every snow pit site to look at vertical variations. A comparison of snow crystal type and EC concentration was done for all 50 samples gathered around Ny-Ålesund. The highest EC concentrations are seen in the lower part of the snow pack, the most metamorphosed snow, and especially in and around ice slabs (see Table 1). Hence, post-depositional processes in the snow pack will alter the initial EC

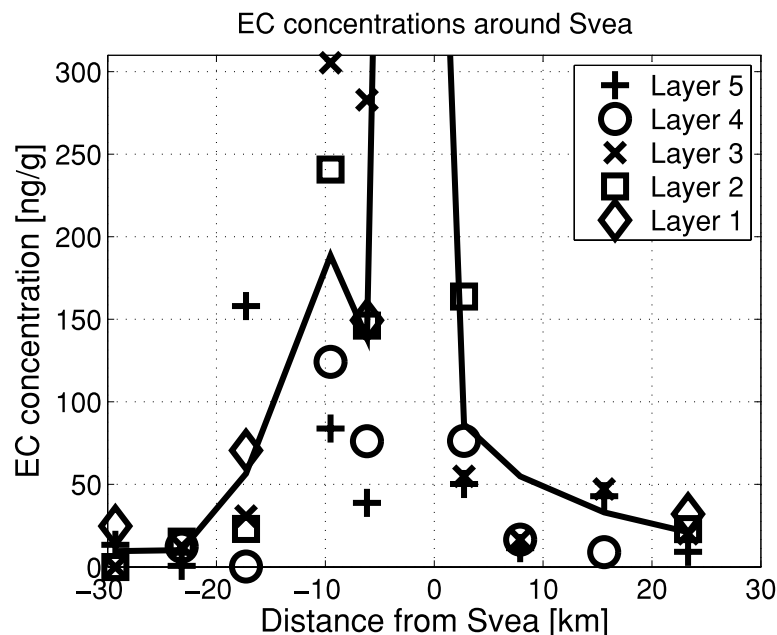


Fig. 6. As Fig. 5, but only for EC concentrations less than  $310 \text{ ng g}^{-1}$ .



Fig. 7. Raw satellite images in the visible from the MODIS Terra satellite showing central Spitsbergen including Svea. The vertical distance is 65 km in the images. Van Mijenfjorden is in the middle of the images. The dates when the images were taken are 4 May, 24 May and 4 June 2008. Extremely high coal dust concentrations are visible around Svea and accelerated snowmelt caused by the high coal dust concentrations is seen in the final image.

concentration (Wania et al., 1998; Jones et al., 2001). We have already seen that EC concentrations were amplified during melt events when melt water drained and the EC particles stayed. Further, the large temperature gradient between the relative warm soil and the relatively cold air will cause an upward vapour transport (Arons and Colbeck, 1995; Jones et al., 2001) while the EC particles are stationary. An increase in EC concentration will also be seen in the surface layer as snow drift will enhance sublimation of snow (Jaedicke, 2001). Hence, EC concentrations tend to increase as more metamorphosed the snow is. Thus, vertical variations of EC in the snow pack will not necessarily render the temporal variability in EC deposition throughout the winter. Post-depositional processes are important for EC concentrations and will, in general, increase the EC concentrations.

### 3.2. EC budget for Svalbard

The estimated EC budget for Svalbard when reduction in snow albedo is considered is given in Table 2. The 'best estimate'

shows that EC pollution from Longyearbyen reduces snow albedo for entire Svalbard with an impact of 2.1% of the total of all EC, while it is 7.9% for Svea. In this estimate, all EC is assumed to have the same optical properties with no differentiation between soot and coal dust particles. The difference in impact is partly explained by the fact that pollution from Svea has a much greater open snow-covered area to impact than pollution from Longyearbyen, due to the wide and long fjords and valleys around Svea. The impact of Ny-Ålesund is set to zero since no clear sign of local pollution was measured around the settlement. Errors in these estimates will depend on errors in the estimated mean EC concentration in the snow pack. In the micro scale study, we observed a standard deviation of 5.9%, while larger variability is expected at lower EC concentrations. If we assume that we have a 40% error in the measurement of EC concentration at every site, the total EC budget has an error of 25%. If local pollution is spread twice the distance as observed and contributing to increased EC concentration in these areas similar to the instrumental detection limit ( $2 \text{ ng g}^{-1}$ ), the EC budget will increase by 14%.



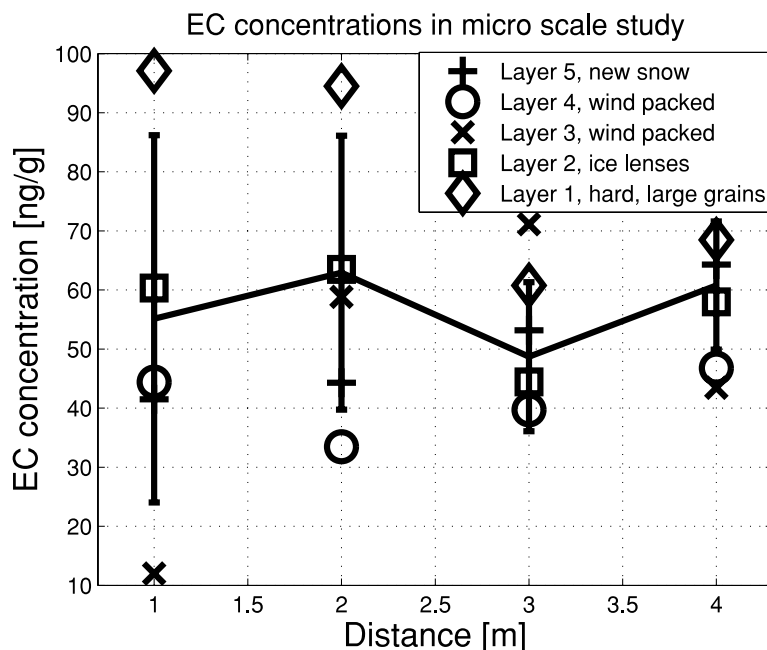


Fig. 8. EC concentrations at the micro scale study.

Table 1. The EC concentration for different snow types for all snow samples gathered around Ny-Ålesund.

| Snow particle type           | EC concentration (ng g <sup>-1</sup> )<br>with standard deviation |
|------------------------------|---|
| Broken and rounded particles | 4.8 ± 4.6   |
| Faceted particles            | 6.4 ± 3.9   |
| Depth hoar                   | 7.2 ± 4.2   |
| Ice                          | 10 ± 2.0  |

Note: These samples are believed to represent the EC background level since no significant local pollution from Ny-Ålesund was found in these samples. The snow has been divided into different groups according to the snow grain type.

In the 'low estimate', we assume coal dust to be 80% less effective at reducing the snow albedo than soot. This reduces the impact of local EC pollution to 0.8% for Longyearbyen and to 1.6% for Svea. This is probably an underestimate since the measured EC around Svea is not only coal dust and we have underestimated the EC concentrations in the most coal dust contaminated areas. Bøggild et al. (2007) measured contaminant content up to 1% of mass in the snow pack along one of the transportation routes. They observed that only small areas, on order of metres from the sources, contained such high concentrations. The measured EC concentrations were much lower, typically four orders of magnitude lower, since the dirtiest samples were not analysed to avoid contamination of the instrumental setup. The error of overestimating the albedo reduction for coal

Table 2. The estimated effect of local EC pollution from Norwegian settlements in Svalbard relative to the albedo reduction caused by all sources of EC for entire Svalbard.

| Settlement   | Low estimate (%) | Best estimate (%) | High estimate (%) | If sea ice (%) |
|--------------|------------------|-------------------|-------------------|----------------|
| Longyearbyen | 0.8              | 2.1               | 3.2               | 8.7            |
| Svea         | 1.6              | 7.9               | 9.8               | 9.8            |
| Ny-Ålesund   | 0                | 0                 | 0                 | 0              |
| Total        | 2.4              | 10                | 13                | 18             |

Note: The best estimate includes only calculations based on site measurements. Some areas that likely are affected were not measured. In the high estimate, these areas are included. 'If sea ice' includes an estimate if Isfjorden was covered by snow covered sea ice.

dust, is, thus, partly cancelled out by underestimating the EC concentration in the most polluted areas.

The 'high estimate' includes areas that are likely contaminated, but where measurements could not be obtained. That will increase the total local impact from 10% to 13%. There was very little sea ice in the Svalbard fjords during the winter of 2007/08. Sea ice covering parts of Isfjorden downwind of Longyearbyen would increase the impact of Longyearbyen significantly. In conclusion, long-range transported EC have a much larger impact than local EC sources for Svalbard. In addition to these Norwegian settlements, the Russian mining town of Barentsburg is another potential big source of local EC. Since no sampling was done near Barentsburg, an estimate for Barentsburg is not given. However, Forsström et al. (2009) measured an EC concentration

of  $240.0 \text{ ng g}^{-1}$  on Linnébreen, 15 km southwest of Barentsburg, which indicates clearly that Barentsburg is a significant source. Svalbard covers less than 0.5% of the Arctic (north of  $70^\circ \text{N}$ ). Thus, the impact of local EC pollution from Svalbard on snow albedo equals to about 0.04% of the impact of all EC in the entire Arctic if the EC background level of the Arctic equals the level in Svalbard.

### 3.3. EC observed from satellite images

In satellite images (MODIS Terra/Aqua), the extremely high EC concentrations around Svea are clearly visible (Fig. 7). The large source of coal dust from the coal stockpile on Cape Amsterdam and the large flat snow covered area around make this a suitable location to study albedo variability connected to high EC concentrations. In the first image, the melting season has just started (4 May 2008) and a coal dust plume can be observed downwind (southwest) of the stockpile. Bøggild et al. (2007) described that melting starts in such areas due to solar radiation before the temperature rises above  $0^\circ \text{C}$ . This melting has led to an increase in the coal dust concentration on the surface in the next image (24 May) making the plume darker and larger in size. On 4 June, the snow is observed to be melted in the plume area, but not in the surrounding area. The accelerated melting is seen all the way out to the open fjord. Hence, coal dust affects the snow melt up to at least 30 km downwind of its source and an area of about  $200 \text{ km}^2$ .

### 3.4. Other light absorbing impurities in the snow

A majority of the filters contained pinkish material after the EC analysis, an indication of a large content of Aeolian sediments in the snow pack. With a typical concentration of  $16 \mu\text{g g}^{-1}$ , as calculated previously, the Aeolian sediment concentration is one order of magnitude larger than the highest EC measurements in this study. However since the Aeolian sediments are mostly non-anthropogenic and less effective at reducing snow albedo than EC (Warren, 1984), these impurities were not included in the modelled albedo impact of contaminants.

## 4. Conclusion

EC pollution from settlements has locally a large impact in Svalbard, while long-range transported EC is dominating when entire Svalbard is considered. The albedo effect of local EC in Norwegian settlements is estimated to be about 10% of the total albedo effect from all sources affecting Svalbard as a whole. Aging of the snow pack and melting are found to alter the EC profiles in the snow. While water vapour will be moved around by post-depositional processes in the snow pack, the EC particles tend to stay in the snow. Elevated EC concentrations were measured around ice lenses and, especially, in the top snow layer during the spring melt. Extremely high EC concentrations are

caused by wind-transported coal dust from coal stockpiles. The dark plumes up to 30 km in length downwind of these stockpiles are clearly visible from satellite images, and these images show accelerated melting in the coal dust affected areas during springtime.

## 5. Acknowledgments

This study was financed by the University Centre in Svalbard (UNIS), University of Oslo (UiO), Svalbard Science Forum (SSF), the Jan Christiansen endowment and the Swedish Research Council FORMAS. We thank the support from students and staff at UNIS and NPI.

## References

- Åkerman, J. H. 1980. *Studies on periglacial geomorphology in West Spitsbergen*. Ph D Thesis, The Royal University of Lund, Lund.
- Arons, E. M. and Colbeck, S. C. 1995. Geometry of heat and mass transfer in dry snow: a review of theory and experiment. *Rev. Geophys.* **33**, 463–493.
- Beine, H. J., Engardt, M., Jaffe, D. A., Hov, Ø., Holmén, K. and co-authors. 1996. Measurements of NO<sub>x</sub> and aerosol particles at the Ny-Alesund Zeppelin mountain station on Svalbard: influence of regional and local pollution sources. *Atmos. Environ.* **30**, 1067–1079.
- Birch, M. E. 2003. Diesel particulate matter (as elemental carbon): method 5040. In: *NIOSH Manual of Analytical Methods*. National Institute of Occupational Safety and Health, Cincinnati, Ohio.
- Birch, M. E. and Cary, R. A. 1996. Elemental carbon-based method for monitoring occupational exposures to particulate diesel exhaust. *Aerosol Sci. Technol.* **25**, 221–241.
- Bond, T. C. and Bergstrom, R. W. 2006. Light absorption by carbonaceous particles: an investigative review. *Aerosol Sci. Technol.* **40** 27–67.
- Bond, T. C., Streets, D. G., Yarber, K. F., Nelson, S. M., Woo, J.-H. and co-authors. 2004. A technology-based global inventory of black and organic carbon emissions from combustion. *J. Geophys. Res.* **109**, D14203, doi:10.1029/2003JD003697.
- Bond, T. C., Habib, G. and Bergstrom, R. W. 2006. Limitations in the enhancement of visible light absorption due to mixing state. *J. Geophys. Res.-Atmos.* **111**, D20211, doi:10.1029/2006JD007315.
- Boots, B. N. 1980. Weighting Thiessen polygons. *Econ. Geogr.* **56**, 248–259.
- Bøggild, C. E., Lüthje, M. and Holmes, J. 2007. Albedo observations with large concentrations of black carbon in High Arctic snow packs from Svalbard. In: *Proceedings of the 64th Eastern Snow Conference*. St. John's, Newfoundland, Canada.
- Chow, J. C., Watson, J. G., Pritchett, L. C., Pierson, W. R., Frazier, C. A. and co-authors. 1993. The direct thermal/optical reflectance carbon analysis system: description, evaluation and applications in U.S. Air quality studies. *Atmos. Environ. A. General Topics* **27**, 1185–1201.
- Chow, J. C., Watson, J. G., Crow, D., Lowenthal, D. H. and Merrifield, T. 2001. Comparison of IMPROVE and NIOSH carbon measurements. *Aerosol. Sci. Technol.* **34**, 23–34.
- Clarke, A. D. and Noone, K. J. 1985. Soot in the Arctic snowpack: a cause for perturbations in radiative transfer. *Atmos. Environ.* **19**, 2045–2053.

- Conway, H., Gades, A. and Raymond, C. F. 1996. Albedo of dirty snow during conditions of melt. *Water Resour. Res.* **32**, 1713–1718.
- Czepe, Z. 1966. The course of the main morphogenetic processes in south-west Spitsbergen. *Prace Geograficzne* **1**, 103–120.
- Eleftheriadis, K., Vratolis, S. and Nyeki, S. 2009. Aerosol black carbon in the European Arctic: measurements at Zeppelin station, Ny-Ålesund, Svalbard from 1998–2007. *Geophys. Res. Lett.* **36**, L02809, doi:10.1029/2008GL035741.
- Flanner, M. G., Zender, C. S., Randerson, J. T. and Rasch, P. J. 2007. Present-day climate forcing and response from black carbon in snow. *J. Geophys. Res.* **112**, D11202, doi:10.1029/2006JD008003.
- Flanner, M. G., Zender, C. S., Hess, P. G., Mahowald, N. M., Painter, T. H. and co-authors. 2009. Springtime warming and reduced snow cover from carbonaceous particles. *Atmos. Chem. Phys.* **9**, 2481–2497.
- Forsström, S., Ström, J., Pedersen, C. A., Isaksson, E. and Gerland, S. 2009. Elemental carbon distribution in Svalbard snow. *J. Geophys. Res.* **114**, D19112, doi:10.1029/2008JD011480.
- Ghose, M. and Majee, S. 2007. Characteristics of hazardous airborne dust around an Indian surface coal mining area. *Environ. Monit. Assess.* **130**, 17–25.
- Grenfell, T. C. and Perovich, D. K. 2004. Seasonal and spatial evolution of albedo in a snow-ice-land-ocean environment. *J. Geophys. Res.* **109**, C01001, doi:10.1029/2003JC001866.
- Grenfell, T. C., Warren, S. G. and Mullen, P. C. 1994. Reflection of solar radiation by the Antarctic snow surface at ultraviolet, visible, and near-infrared wavelengths. *J. Geophys. Res.* **99**, 18 669–18 684.
- Grenfell, T. C., Light, B. and Sturm, M. 2002. Spatial distribution and radiative effects of soot in the snow and sea ice during the SHEBA experiment. *J. Geophys. Res.* **107**, 8032, doi:10.1029/2000JC000414.
- Hagen, J. O. and Liestøl, O. 1990. Long-term glacier mass-balance investigations in Svalbard, 1950–88. *Ann. Glaciol.* **14**, 102–106.
- Hagler, G. S. W., Bergin, M. H., Smith, E. A., Town, M. and Dibb, J. E. 2008. Local anthropogenic impact on particulate elemental carbon concentrations at Summit, Greenland. *Atmos. Chem. Phys.* **8**, 2485–2491.
- Hansen, J., Sato, M., Ruedy, R., Nazarenko, L., Lacis, A. and co-authors. 2005. Efficacy of climate forcings. *J. Geophys. Res.* **110**, D18104, doi:10.1029/2005JD005776.
- Jaedicke, C. 2001. *Drifting snow and snow accumulation in complex Arctic terrain: field experiments and numerical modelling*. PhD Thesis, University of Bergen, Bergen. <http://worldcat.org/oclc/50333174>.
- Jaedicke, C. 2002. Snow drift losses from an Arctic catchment on Spitsbergen: an additional process in the water balance. *Cold Reg. Sci. Technol.* **34**, 1–10.
- Jones, H. G., Pomeroy, J. W., Walker, D. A. and Hoham, R. W. 2001. *Snow Ecology: An Interdisciplinary Examination of Snow-Covered Ecosystems*, Cambridge University Press, Cambridge, UK.
- Jones, T., Blackmore, P., Leach, M., Bérubé, K., Sexton, K. and co-authors. 2002. Characterisation of airborne particles collected within and proximal to an opencast coalmine: South Wales, U.K. *Environ. Monit. Assess.* **75**, 293–312.
- Law, K. S. and Stohl, A. 2007. Arctic air pollution: origins and impacts. *Science* **315**, 1537–1540.
- Male, D. H. 1980. The seasonal snowcover. In: *Dynamics of Snow and Ice Masses*. (ed. Colbeck, S. C.). Academic Press, New York, 305–395.
- Myhr, K. A. 2003. *Dust in working environment and outer environment in Svea (Støv i arbeidsmiljø og ytre miljø i Svea)*. Diploma Thesis. Department, Norwegian University of Science and Technology, Trondheim, Norway.
- Naidoo, G. and Chirkoot, D. 2004. The effects of coal dust on photosynthetic performance of the mangrove, *Avicennia marina* in Richards Bay, South Africa. *Environ. Pollut.* **127**, 359–366.
- Ogren, J. A., Charlson, R. J. and Groblicki, P. J. 1983. Determination of elemental carbon in rainwater. *Anal. Chem.* **55**, 1569–1572.
- Owens, P. N. and Slaymaker, O. 1997. Contemporary and post-glacial rates of aeolian deposition in the coast mountains of British Columbia, Canada. *Geogr. Ann. A.* **79**, 267–276.
- Quinn, P. K., Bates, T. S., Baum, E., Doubleday, N., Fiore, A. M. and co-authors. 2008. Short-lived pollutants in the Arctic: their climate impact and possible mitigation strategies. *Atmos. Chem. Phys.* **8**, 1723–1735.
- Reddy, M. S. and Boucher, O. 2007. Climate impact of black carbon emitted from energy consumption in the world's regions. *Geophys. Res. Lett.* **34**, L11802, doi:10.1029/2006GL028904.
- Reimann, S., Kallenborn, R. and Schmidbauer, N. 2009. Severe aromatic hydrocarbon pollution in the Arctic Town of Longyearbyen (Svalbard) caused by snowmobile emissions. *Environ. Sci. Technol.* **43**, 4791–4795.
- Reisinger, P., Wonaschütz, A., Hitznerberger, R., Petzold, A., Bauer, H. and co-authors. 2008. Intercomparison of measurement techniques for black or elemental carbon under urban background conditions in wintertime: influence of biomass combustion. *Environ. Sci. Technol.* **42**, 884–889.
- Rosen, H., Novakov, T. and Bodhaine, B. A. 1981. Soot in the Arctic. *Atmos. Environ.* **15**, 1371–1374.
- Rypdal, K., Rive, N., Berntsen, T. K., Klimont, Z., Mideksa, T. K. and co-authors. 2009. Costs and global impacts of black carbon abatement strategies. *Tellus* **61B**, 625–641.
- Schulz, M., Textor, C., Kinne, S., Balkanski, Y., Bauer, S. and co-authors. 2006. Radiative forcing by aerosols as derived from the AeroCom present-day and pre-industrial simulations. *Atmos. Chem. Phys.* **6**, 5225–5246.
- Shaw, G. E. 1995. The Arctic haze phenomenon. *Bull. Am. Meteorol. Soc.* **76**, 2403–2413.
- Shindell, D. T., Chin, M., Dentener, F., Doherty, R. M., Faluvegi, G. and co-authors. 2008. A multi-model assessment of pollution transport to the Arctic. *Atmos. Chem. Phys.* **8**, 5353–5372.
- Stamnes, K., Tsay, S. C., Wiscombe, W. and Jayaweera, K. 1988. Numerically stable algorithm for discrete-ordinate-method radiative transfer in multiple scattering and emitting layered media. *Appl. Opt.* **27**, 2502–2509.
- Stohl, A. 2006. Characteristics of atmospheric transport into the Arctic troposphere. *J. Geophys. Res.* **111**, D11306, doi:10.1029/2005JD006888.
- Tedesco, L., Vichi, M., Haapala, J. and Stipa, T. 2009. An enhanced sea-ice thermodynamic model applied to the Baltic Sea. *Boreal Environ. Res.* **14**, 68–80.
- Vestreng, V., Kallenborn, R. and Økstad, E. 2009. Norwegian Arctic climate: climate influencing emissions, scenarios and mitigation options at Svalbard. *Climate and Pollution Agency*, TA-2552.
- Vignati, E., Karl, M., Krol, M., Wilson, J., Stier, P. and co-authors. 2010. Sources of uncertainties in modelling black carbon at the global scale. *Atmos. Chem. Phys.* **10**, 2595–2611.

- Wania, F., Hoff, J. T., Jia, C. Q. and Mackay, D. 1998. The effects of snow and ice on the environmental behaviour of hydrophobic organic chemicals. *Environ. Pollut.* **102**, 25–41.
- Warren, S. G. 1984. Impurities in snow: effects on albedo and snowmelt. *Ann. Glaciol.* **5**, 177–179.
- Warren, S. G. and Clarke, A. D. 1990. Soot in the atmosphere and snow surface of Antarctica. *J. Geophys. Res.* **95**, 1811–1816.
- Warren, S. G. and Wiscombe, W. J. 1980. A model for the spectral albedo of snow. II: snow containing atmospheric aerosols. *J. Atmos. Sci.* **37**, 2734–2745.
- Watson, J. G., Chow, J. C. and Chen, L.-W. A. 2005. Summary of organic and elemental carbon/black carbon analysis methods and intercomparisons. *Aerosol Air. Qual. Res.* **5**, 65–102.
- Winther, J.-G., Bruland, O., Sand, K., Killingtveit, Å. and Marechal, D. 1998. Snow accumulation distribution on Spitsbergen, Svalbard, in 1997. *Polar Res.* **17**, 155–164.